International Journal of Mechanical Engineering and Applications
2021; 9(2): 33-41
http://www.sciencepublishinggroup.com/j/ijmea
doi: 10.11648/j.ijmea.20210902.11
ISSN: 2330-023X (Print); ISSN: 2330-0248 (Online)

An Optimization Method for Thermal Convex Deformation of Machine Tool's Guideway Based on the Conservation of Energy

Ruoda Wang, Kaiguo Fan*, Qiang Li, Yifei Li

School of Mechanical Engineering, University of Shanghai for Science and Technology, Shanghai, China

Email address:

ruoda_wang@163.com (Ruoda Wang), fkg11@163.com (Kaiguo Fan)

*Corresponding author

To cite this article:

Ruoda Wang, Kaiguo Fan, Qiang Li, Yifei Li. An Optimization Method for Thermal Convex Deformation of Machine Tool's Guideway Based on the Conservation of Energy. *International Journal of Mechanical Engineering and Applications*. Vol. 9, No. 2, 2021, pp. 33-41.
doi: 10.11648/j.ijmea.20210902.11

Received: March 9, 2021; **Accepted**: April 8, 2021; **Published**: April 12, 2021

Abstract: With the improvement of machining accuracy and efficiency, heat generation of guideway becomes the crucial problem which will cause thermal convex deformation. Thermal convex deformation of guideway which accounts for about 22.7% of the total errors is one of the main factors affecting the machining accuracy of machine tool. A conservation of energy-based optimization method is proposed to balance the temperature field and reduce the thermal convex deformation. The main strategy of this method is to transfer the heat from high temperature regions to the lower temperature regions through a heat transfer system. The structure and contact area of the heat transfer system are determined according to the output and input heat ratio of the guideway. The simulation and experimental results show that the temperature field of the guideway is more uniform after optimized, the thermal convex deformation is reduced about 50%, it is of great significance to reduce the thermal convex deformation of the guideway and improve the machining accuracy of machine tool.

Keywords: Conservation of Energy, Thermal Optimization, Temperature Distribution, Thermal Convex, Guideway

1. Introduction

The guideway is the benchmark used to determine the relative position of the worktable and spindle in a machine tool. In high-speed and high-precision machining, the high-speed rotation of spindle and movement of feed system will generate a large amount of friction heat and produce the thermal deformation which seriously affect the machining accuracy of machine tool. Research shows that machining errors caused by thermal deformation account for 40% to 70% of the total errors in precision machining [1]. Yun [2] studied the thermal characteristics of the guideway and ball screw of CNC machine tool based on the finite element method, it was found that the thermal error of guideway accounts for about 22.7% of the total errors of machine tool. Therefore, studying and optimizing the thermal deformation of machine tool's guideway is of great significance for improving the machining accuracy of machine tool.

In the existing research, there are mainly two methods to reduce the thermal error, one is the thermal error compensation method [3, 4], and the other is thermal error prevention method. The error compensation method is that it uses the software to real-timely compensate the thermal errors without changing the machine tool's structure [5]. Barakat et al. [6] proposed an error compensation method for kinematics and geometric errors in a coordinate measuring machine which can effectively improve the accuracy of the coordinate measuring instrument. Chen [7] developed a kinematics modeling and a post-processing method to implement the real-time error compensation for the kinematics errors on a five-axis CNC machine tool.

The thermal error prevention method is to control the thermal deformation or temperature rise directly through changing the machine tool's structure or cooling the internal heat sources and its assemblies. Thermal optimization design is one of the mainly used thermal error prevention method. The main strategy is to design a symmetrical structure to reduce the radial thermal deformation, or using the constraint

method to limit the thermal deformation, or transfer the thermal deformation to the direction which does not influence the machining accuracy [8-10]. The other thermal error prevention method is to control the temperature rise of assemblies of machine tool, and the cooling system becomes the best choice. Xia et al. [11] designed a fractal tree-like channel network radiator in the spindle cooling system based on fractal theory, and verified the heat dissipation of the device through experiments. Li et al. [12] used a single-circuit thermosyphon to cool the spindle, the temperature rise is controlled at 28.5°C.

In the above-mentioned research, numerical simulation technology is usually used to discuss the main factors affecting the temperature field and thermal deformation of machine tool to provide a basis for thermal error compensation and prevention. Guo et al. [13] analyzed the main factors affecting the deformation of guideway using the finite element method. Zeng et al. [14] discussed the influence of thermal deformation of guideway in the axial direction on the machining accuracy of workpiece through thermal-structure coupling analysis.

In addition to the above-mentioned researches, some other studies are carried out related to the thermal deformation control. Kang et al. [15] built a thermal error model using the neural network method and studied the relevant factors affecting the thermal error. Hiroshi et al. [16] used the approximate thermal deformation method to improve the machining accuracy of machine tool. Li et al. [17] established a finite element objective function for thermal error of guideway, and optimized the boundary conditions of finite element model using the response surface approximation model method to improve the machining accuracy of machine tool. Zhou et al. [18] used the fast heat conduction method to balance the temperature field of spindle housing, and the thermal tilt of the spindle was greatly reduced.

All the thermal error control method can effectively reduce the thermal deformation of machine tool. However, there is no research involving the prevention of thermal deformation of guideway. In this paper, the thermal convex deformation of guideway is studied and optimized using the principle of conservation of energy. The main idea of the proposed method is to transfer the heat from higher temperature regions to lower temperature regions to balance the temperature field of guideway and to reduce the thermal convex deformation. Section 2 introduces the optimization mechanism and design strategy of heat transfer system. Section 3 is the simulation and optimization strategy of the guideway. Section 4 verifies the optimization effect through experiments, and the experimental results show that the thermal convex deformation of the guideway is reduced about 50% using the proposed thermal error optimization method. Finally, some conclusions are given in section 5 based on the simulation and experimental results.

2. Optimization Mechanism

The main idea of the proposed thermal optimization method is to transfer the heat from higher temperature regions to the lower temperature regions to balance the temperature distribution of guideway according to the principle of conservation of energy. The key of this method is to determine the heat need to be transferred and to design the heat transfer system.

2.1. Calculation the Output and Input heat

As shown in Figure 1, a part of the frication heat generated by guideway transfers to the ambient through convection, a part of it transfers to the worktable and machine bed through conduction which causes the temperature rises of the components. Due to the influence of the location of heat sources and the heat transfer process, the temperature distribution of the guideway is uneven as shown in Figure 2 which will cause the convex deformation and affect the machining accuracy of machine tool. In order to balance the temperature distribution of the guideway and to reduce the convex deformation, the heat in the higher temperature regions should transfer to the lower temperature regions. The total heat in the guideway can be calculated as,

$$Q_g = 9.8 c_g \rho_g S_g \int_0^l f_c(x) \tag{1}$$

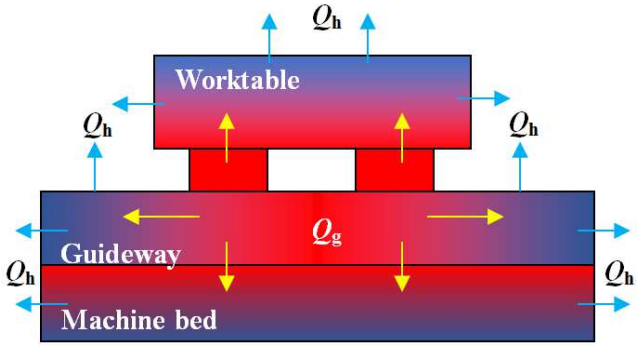

Figure 1. *Heat transfer diagram of guideway.*

where, Q_g is the heat generated by the guideway, Q_h is the heat convection, c_g and ρ_g are the specific heating capacity in J/(kg°C) and density in kg/m^3 of the guideway, respectively, S_g is the cross-sectional area of the guideway in m^2, $f_c(x)$ is the temperature rise function of the guideway, l is the length of the guideway in meter.

The balance of the temperature distribution is to obtain a uniform temperature rise along the axial direction of the guideway, therefore, the linear fitting of the temperature rise should be established as,

$$f_l(x) = p_1 x + p_2 \tag{2}$$

where, p_1 and p_2 are the coefficients.

As shown in Figure 2, the temperature distribution of the guideway along the axial direction is separated into 4 regions by the linear fitting curve and marked as Q_1, Q_2, Q_3, and Q_4. The total heat in the guideway is $Q_g = Q_1 + Q_4$. In order to balance the heat along the axial direction of the guideway, the

heat in the higher temperature region Q_1 needs to be quickly transferred to the lower temperature regions Q_2 and Q_3 through the high thermal conductivity material. That is to say, the transferred heat Q_1 should equal to Q_2 and Q_3,

$$Q_1 = Q_2 + Q_3 \tag{3}$$

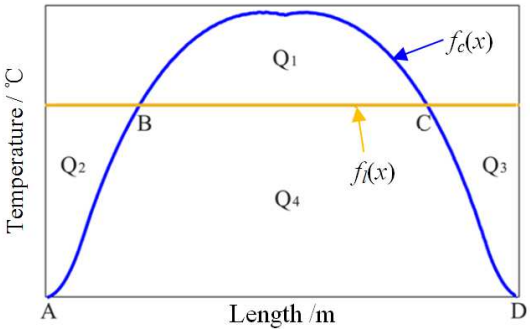

Figure 2. *Temperature distribution of guideway.*

Figure 2. $f_c(x)$ is the temperature rise of the guideway, $f_l(x)$ is the linear fitting of temperature rise, Q_1, Q_2, Q_3, and Q_4 are 4 heat regions, A and D are two ends of the guideway, B and C are the intersections of $f_c(x)$ and $f_l(x)$.

To transfer the heat from higher temperature regions to the lower temperature regions, a heat transfer system with high thermal conductivity is designed in section 2.2. Since the heat transfer system is connected with the guideway through thermal silica gel, the thermal contact resistance is very small and can be ignored.

Assuming that the heat dissipation rate of the system is unchanged after using the heat transfer system, then, Eq. 3 can be rewritten as Eq. 4 according to the conservation of energy.

$$\begin{aligned}&\int_B^C C_g m_g \left(f_c(x) - f_l(x)\right) dx = \\ &\int_A^B C_g m_g \left|f_c(x) - f_l(x)\right| dx + \int_C^D C_g m_g \left|f_c(x) - f_l(x)\right| dx\end{aligned} \tag{4}$$

In Eq. 4, the increase of internal energy of the heat transfer system is ignored due to it is only a heat transfer medium when the system is in thermal equilibrium. For a given guideway, the temperature rise is related to the heat generation, but the temperature distribution trend is basically the same when the working stroke of the machine tool remains unchanged especially in batch machining. Therefore, the heat ratio of output and input along the axial direction of the guideway can be calculated using the following calculation process.

1) The first step is to obtain the temperature rise curve using the temperature sensors to measure the temperature rise along the axial direction or using the finite element method to simulate the temperature distribution of the guideway, the obtained temperature rise curve is marked as $f_c(x)$ as shown in Figure 2.

2) The second step is to establish the linear fitting model using the least squares method as shown in Eq. 2, and then using the following formula to revise the parameter p_2, the revised linear fitting function is marked as $f_l(x)$ as shown in Figure 2.

$$\int_0^l f_c(x) - \frac{1}{2} p_1 l^2 - p_2 l = 0 \tag{5}$$

where, l is the length of guideway in meter.

3) The third step is to calculate the coordinates of intersections of the temperature rise curve and the new linear fitting line, which is marked as B and C as shown in Figure 2.

4) The fourth step is using Eq. 4 to calculate the output heat Q_1 and the input heat Q_2 and Q_3. And the calculated results are used to calculate the heat ratio by the next step.

5) The fifth step is to calculate the heat ratio using the following formula,

$$\eta_i = \frac{Q_i}{2\int_B^C C_g m_g \left(f_c(x) - f_l(x)\right) dx} \tag{6}$$

where, $Q_i = \int_{l_i}^{l_{i+1}} C_g m_g \left|f_c(x) - f_l(x)\right| dx$ is the subdivision of the transferred heat as shown in Figure 3, l_i and l_{i+1} are the subdivision interval which can be determined through the required heat transfer accuracy, for example, high heat transfer accuracy requires a smaller subdivision interval, and vice versa.

Using the above-mentioned method, the subdivided heat ratio of output and input can be calculated. After determining the heat ratio of output and input, next is using the heat ratio to design the heat transfer system.

2.2. Design the Heat Transfer System

In order to transfer the heat quickly, the copper alloy with high thermal conductivity is selected as the heat transfer material in this study. Since the heat outputted from the higher temperature region Q_1 should be transferred to the heat transfer system firstly, and then transferred to the lower temperature regions Q_2 and Q_3, the heat transferred to the heat transfer system is equal to the heat outputted from the guideway when the system is in thermal equilibrium. Then, the required quality and volume of the high thermal conductivity material can be calculated as,

$$\begin{cases}\int_0^l C_h m_h \Delta t = \int_B^C C_g m_g \left(f_c(x) - f_l(x)\right) dx \\ m_h = \rho_h V_h\end{cases} \tag{7}$$

where, C_h is the specific heat capacity of the high thermal conductivity material in J/(kg°C), m_h and m_g denote the quality of the high thermal conductivity material and the guideway in kg, respectively, ρ_h is density of the copper alloy in kg/m^3.

Since C_h, C_g, m_g, and ρ_h are all known, the quality and volume of the high thermal conductivity material can be calculated through Eq. 7. Next is to calculate the contact area between the heat transfer system and the guideway using Eq. 8.

$$A_i = \eta_i \times A_{\text{upper}} \tag{8}$$

where, A_{upper} is the area of the upper surface of the guideway in m^2.

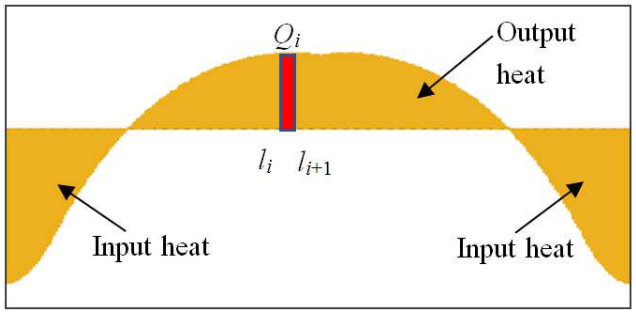

Figure 3. *The output and input heat in guideway.*

Figure 3. Q_i is subdivision of the transferred heat, l_i and l_{i+1} are the subdivision interval.

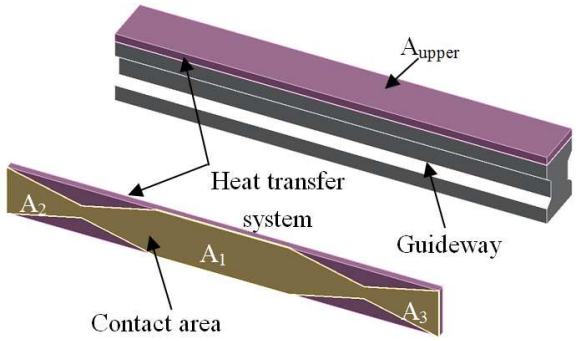

Figure 4. *The heat transfer system.*

Using Eq. 8, the required contact area between the heat transfer system and the guideway at heat transfer regions A_1, A_2, and A_3 can be determined as shown in Figure 4. The heat in the guideway at region Q_1 is transferred to the copper alloy through the contact area A_1, then it conducts quickly in the copper alloy and form a uniform temperature field. Thereby the temperature in the copper alloy at the regions Q_2 and Q_3 will higher than the guideway at the same regions, then the heat in the copper alloy will transfer to the guideway through the contact area A_2 and A_3 to form a uniform temperature field.

Using the aboved-mentioned thermal optimization method, the heat ratio needs to be outputted and inputted can be determained according to the principle of conservation of energy, and the heat transfer system can be designed using heat ratio subdivision method. In order to verify this method, the thermal behavior of a guideway is simulated and optimized in section 3.

3. Simulation and Optimization

3.1. Simulation

In this paper, a guideway with dimensions of 1180×23×22 mm is used to study the thermal behavior and its optimization as shown in Figure 5. The material of the guideway is carbon steel, and its material properties are shown in Table 1. The guideway is fixed on the machine bed by bolts. In order to simulate the thermal behavior of the guideway, the boundary conditions should be calculated firstly. The heat of the guideway is usually generated by the frication between the slider and the guideway, which can be calculated as,

$$Q = \frac{\mu F v}{J} \tag{9}$$

where, μ=0.05 is the friction coefficient between the slider and the guideway, F=2000 N is the pressure applied on the guideway, v=0.5 m/s is the relative moving speed between the slider and the guideway, J=4.2 J/cal is the thermal power equivalent. Therefore, the heat generation of the guideway can be calculated as Q=11.9 W, and the heat flux of the contact surface between the slider and the guideway is 6159.4 W/m^2.

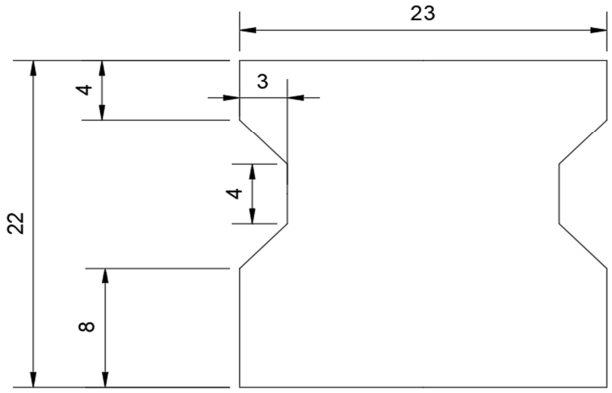

Figure 5. *The cross-section of the guideway.*

When the air flows through the surface of the guideway, the process of heat transfer between the two is called convection. This process includes the convection of fluid macroscopic displacement and the heat conduction between fluid molecules, which is the result of the combined action of convection and heat conduction. This is the main heat dissipation form of the guideway, and the heat convection coefficient can be calculated as,

$$h = \frac{Nu \cdot \lambda}{L} \tag{10}$$

where, Nu is the Nusselt number, λ is the thermal conductivity of the fluid in W/(m·k), L is the geometric feature size in meter.

Since the heat transfer at the surface of the guideway belongs to natural convection, the Nusselt number can be calculated as,

$$\begin{cases} Nu = C(Gr \cdot \Pr)_m^n \\ Gr = \dfrac{g\beta\Delta t L^3}{v^2} \end{cases} \tag{11}$$

where, Gr is the Grashof number, Pr is the Prandtl number, g is the acceleration of gravity in m/s^2, β is the volume expansion coefficient in 1/k, Δt is the temperature difference between the fluid and the wall in °C, v is the kinematic viscosity, the subscript m represents the qualitative temperature, c and n are constants. Then, the heat convection coefficient of the guideway is calculated as h=7.6 W/(m^2·k).

Table 1. *Material properties of the guideway.*

Physical property	Value
Thermal Conductivity in w/m·K	55
Elastic Modulus in Gpa	12
Poisson's ratio	0.3
Thermal expansion coefficient in m/K	1.2×10^{-5}
Specific heat capacity in J/kg·K	470
Density in kg/m^3	7.8×10^{3}

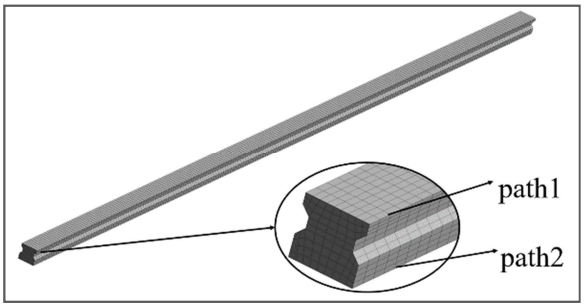

Figure 6. *Finite element model of the guideway.*

Figure 6 shows the finite element model of the guideway, the chamfers and holes on the guideway are removed. Path1 and path2 represent the edges at the top and bottom of the guideway. Because the heat source of guideway is motive, the moving heat source is applied to the finite element model. The initial and reference temperature is set as 20 °C, the heat convection is applied on the surface of the guideway, the simulation time is 14400 seconds. Using the Ansys software, the temperature field and the thermal deformation of the guideway can be simulated.

Figure 7 shows the temperature field of the guideway at 14400 seconds. It can be seen from Figure 7 that the higher temperature region is occurred in the middle of the guideway, the maximum temperature is 26.051°C. The lower temperature regions are occurred in both ends of the guideway, and the minimum temperature is 24.29°C. The temperature distribution is uneven.

Figure 8 shows the temperature rise at the midpoint of the guideway. It can be seen from Figure 8 that the temperature at the midpoint rises sharply first and then stabilizes at 14400s. At this time, the temperature field of the guideway reaches a steady-state. The trends of the temperature rise curves at the other points are similar to the midpoint, but the temperature rises are different.

Applying the transient temperature field at 14400 seconds and the displacement constraint to the finite element model, the thermal deformation of the guideway can be simulated through thermal-structure coupling analysis and the simulation result is shown in Figure 9. The maximum thermal deformation of the guideway in the Y-direction is 2.2525 μm. The thermal deformation trend of the guideway is convex.

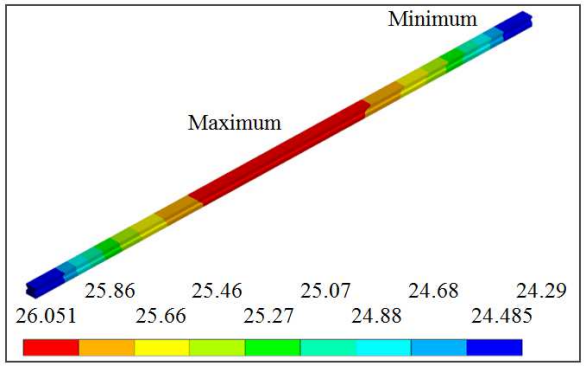

Figure 7. *Temperature field of the guideway.*

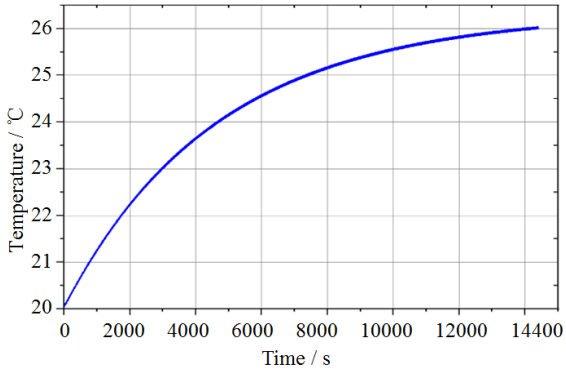

Figure 8. *The temperature rises at the midpoint.*

Using the numerical simulation method, the temperature field and thermal deformation of a single guideway can be obtained. However, the guideway is fixed on the machine bed in actual situation, the heat conduction between the guideway and machine bed as well as the influence of thermal deformation of machine bed on the guideway should be considered.

Because the heat transfer between the guideway and machine bed is heat conduction, the thermal contact resistance should be calculated firstly to simulate the thermal behavior when the guideway is fixed on the machine bed. The thermal contact resistance can be calculated as [19],

$$R_c = \frac{\sigma}{105.6\times k}\times\left(\frac{H}{P}\right)^{0.618} \tag{12}$$

where, σ is the root-mean-square value of surface roughness which can be calculated through Eq. 13, k is the tuned average thermal conductivity which can be calculated by Eq. 14, H is the minimum hardness of the contact surfaces in HB, P is the contact pressure in MPa, which can be calculated by Eq. 15.

$$\sigma = \sqrt{\sigma_1^2 + \sigma_2^2} \tag{13}$$

where, σ_1 and σ_2 are the surface roughness of the two contact parts in macron.

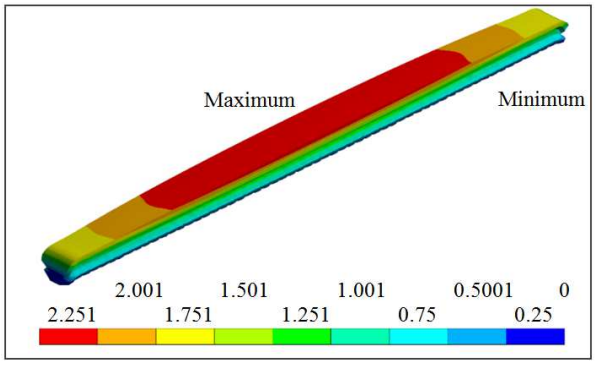

Figure 9. *Thermal deformation of the guideway.*

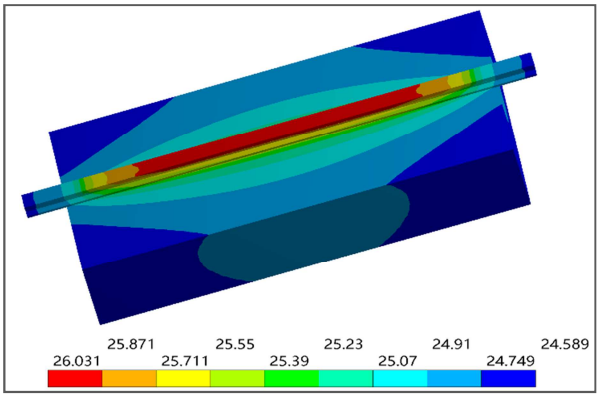

Figure 10. *Temperature field of the guideway and machine bed.*

$$k = \frac{2k_1k_2}{k_1 + k_2} \tag{14}$$

where, k_1 and k_2 are the thermal conductivities of the two contact parts in W/(m·K).

$$p = F / S \tag{15}$$

Applying the boundary conditions to the finite element model when the guideway is fixed on the machine bed, the temperature field and thermal deformation can be simulated using the Ansys. The temperature field is shown in Figure 10, the maximum temperature is 26.031°C which is basically consistent with the temperature field when the guideway is single. The maximum thermal deformation along the Y-direction of the guideway is 10.923 μm when the guideway is fixed on the machine bed as show in Figure 11, which is much higher than the maximum thermal deformation when the guideway is single. This is because the thermal deformation of the machine bed is superimposed on the guideway. Therefore, it is very important to control and optimize the thermal deformation of the guideway.

3.2. Optimization of the Temperature Field

Figure 12 shows the temperature rises curves of path 1 and path 2 along the axial direction. The temperature trends of these two paths are almost the same, and the maximum temperature difference between the two is only 0.015°C. It represents that the transient temperature of the guideway has reached the steady-state.

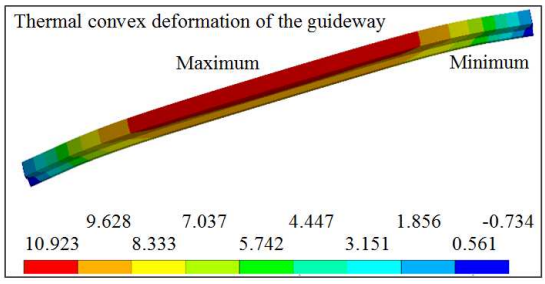

Figure 11. *Thermal deformation along the Y-direction.*

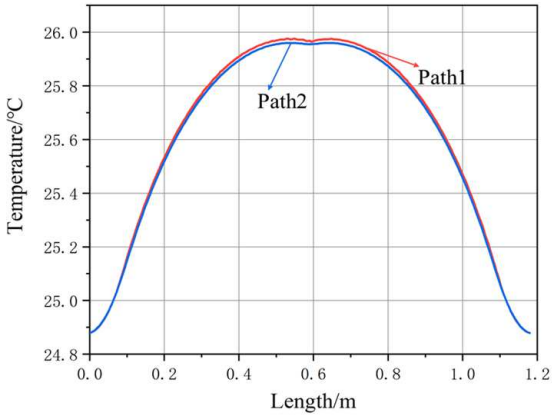

Figure 12. *Axial temperature distribution of path1 and path2.*

The temperature distribution along the axial direction of the guideway can be obtained through calculating the average temperature rise of path 1 and path 2 as shown in Figure 13 (curve $T(X)$). Using the least square fitting method, a sixth-order polynomial can be obtained as shown in Eq. 16.

$$T(x) = 31.22x^6 - 110.5x^5 + 146.1x^4 - 88.37x^3 + 20.33x^2 + 1.81x + 24.85 \tag{16}$$

In Eq. 16, the fitting error of the temperature rise of the guideway is 0.02373, the root mean square error is 0.009427, the coefficient of determination of the equation is 0.9993. That is to say, the sixth-order polynomial can appropriately express the temperature distribution along the axial direction of the guideway. The linear fitting of the temperature rise of the guideway can be obtained using Eqs. (2, 5) as shown in Figure 13 (curve $G(X)$). The intersections of the linear fitting and the temperature rise curve is marked as J and K as shown in Figure 13, and the coordinates of intersections J and K can be calculated as J (0.23, 25.61), K (0.94, 25.6) using Eq. 17.

$$\begin{cases} 31.22x^6 - 110.5x^5 + 146.1x^4 - 88.37x^3 + 20.33x^2 + \\ 1.81x + 24.85 = -0.014x + 25.62 \quad (0 < x < 1.18) \end{cases} \tag{17}$$

In order to transfer the heat from the higher temperature region Q_1 to the lower temperature regions Q_2 and Q_3 quickly, the material with high thermal conductivity should be selected. Currently, materials with high thermal conductivity include

the diamond, carbon fiber, copper alloys, aluminum alloys, etc. Considering the factors of processability and price, the copper alloy with thermal conductivity of λ=399 W/(m·K) is selected as the heat transfer medium in this study. Substituting the material properties of the copper alloy and the guideway as shown in Table 1 into Eq. 4, the output and input heat can be calculated as shown in Eq. 18.

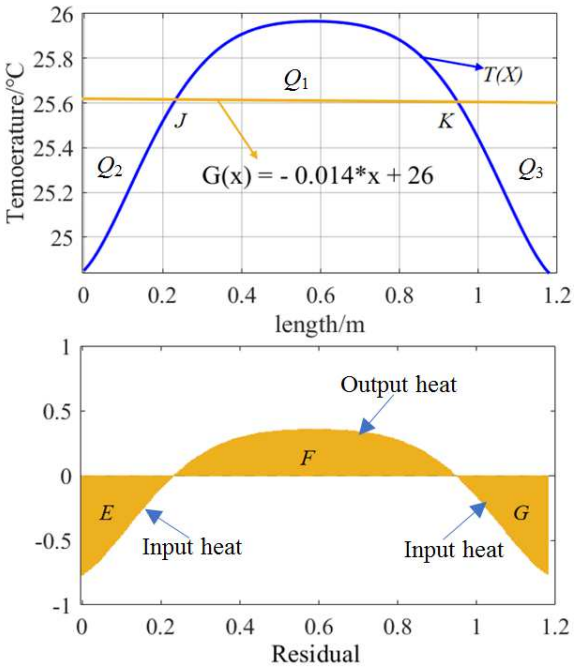

Figure 13. *Temperature distribution and its linear fitting.*

Figure 13. $T(X)$ is the temperature rise of the guideway, $G(X)$ is the linear fitting of the temperature rise, Q_1 is the output heat region, Q_2 and Q_3 are the input heat region, J, K is the intersections of $T(X)$ and $G(X)$.

$$\begin{cases} Q_1 = \int_{0.23}^{0.93} 0.46\times10^3\times3.59\times[T(x)-G(x)]dx \\ \quad =306.69\ \text{J} \\ Q_2 = \int_{0}^{0.23} 0.46\times10^3\times3.59\times[G(x)-T(x)]dx \\ \quad =151.92\ \text{J} \\ Q_3 = \int_{0.93}^{1.18} 0.46\times10^3\times3.59\times[G(x)-T(x)]dx \\ \quad =151.78\ \text{J} \end{cases} \tag{18}$$

Substituting Q_1, Q_2 and Q_3 into Eq. 6, the heat ratio of output and input of the guideway can be calculated as η_1=50%, η_2=24.76%, and η_3=25.24%. Substituting η_1, η_2, and η_3 into Eq. 8, the contact area between the guideway and the copper alloy at regions E, F, and G as shown in Figure 13 can be calculated as S_E=13.1 cm^2, S_F=81.95 cm^2, and S_G =19.93 cm^2. The subdivision of the contact area of E, F, and G can be calculated using Eq. 6. Figure 14 shows the simplified structure of the heat transfer system. In Figure 14, S_E, S_F, and S_G express the contact areas between the guideway and the copper alloy which can be connected by thermal conductive silicone.

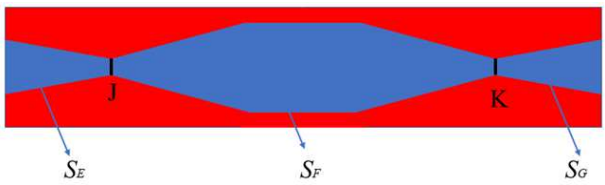

Figure 14. *The shape of the heat transfer system.*

Figure 14. S_E, S_F, and S_G are the contact areas between the guideway and the copper alloy.

Substituting the properties of the copper alloy into Eq. 7 the weight of the required copper alloy can be calculated as m_h=4.23 kg, the volume can be calculated as V_h=4.72×10^{-4} m^3 as shown in Eq. 19.

$$\begin{cases} \int_{0.23}^{0.93} 0.39\times10^3\times m_h[T(x)-G(x)]dx = \\ \int_{0.23}^{0.93} 0.46\times10^3\times3.59\times[T(x)-G(x)]dx \\ 8.96\times10^3\times V_h = 4.23 \rightarrow V_h = 4.72\times10^{-4}\ \text{m}^3 \end{cases} \tag{19}$$

Using the optimization method for thermal convex deformation of guideway, a heat transfer system can be obtained as shown in Figure 14. In order to verify the effectiveness of the prosed optimization method, the experiments is carried out in section 4.

4. Experimental Verification

4.1. Experimental Setup

Because the slider moves when the guideway works, it is difficult to arrange the sensors on the guideway to measure the temperature and thermal deformation. We designed a thermal behavior testing platform as shown in Figure 15 (1). The testing platform includes a machine bed, a single guideway, four adjustable heaters, a heat transfer system, and a data acquisition system. The guideway is fixed on the machine bed through bolts, the adjustable heaters are attached on the surface of the guideway to simulate the friction heat. Six temperature sensors and five eddy current displacement sensors are used to measure the temperature and thermal deformation of the guideway before and after optimized. The installation sequence of the temperature sensors from left to right is T1, T2, T3, T4, T5, and T6 as shown in Figure 15 (2) and (4). The installation sequence of the eddy current displacement sensors from left to right is D1, D2, D3, D4, and D5 as shown in Figure 15 (2) and (4).

The heaters are evenly arranged in the stroke of the sliders. The power of each heater is adjusted to a suitable value according to the calculation result of the friction heat of the guideway. The room temperature is around 29°C. The experiment time is 7200 seconds. Figure 16 shows the experimental results of the guideway before and after optimized.

4.2. Experimental Results

Figure 16(a) shows the temperature rises of the guideway before optimized, the temperature rises marked as Tem1 to Tem6 are measured by the temperature sensors T1 to T6. Because both ends of the guideway hang in the air, its convective heat transfer is much larger than the middle part. Therefore, the temperature rise at both ends of the guideway is not considered in this study. After heating for 2 hours, the maximum temperature rise is about 8°C which occurred in the middle of the guideway, the maximum temperature difference is about 4°C.

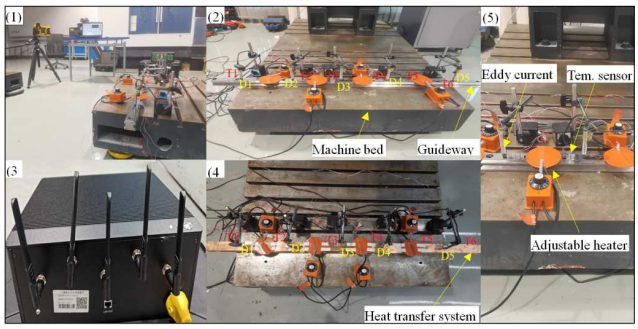

Figure 15. *Experimental setup. (1) Thermal behavior testing platform of guideway, (2) Experimental setup before optimization, (3) Data acquisition device, (4) Experimental setup with heat transfer system, (5) Temperature and displacement sensors arrangement.*

Figure 15. T1, T2, T3, T4, T5, and T6 are the temperature sensors, D1, D2, D3, D4, and D5 are the eddy current displacement sensors.

Figure 16(b) shows the temperature rises of the guideway with optimized, after heating for 2 hours, the maximum temperature rise is about 8°C which occurred in the middle of the guideway and is similarly to the maximum temperature rise of the guideway before optimized. Except for the temperature rises of both ends of the guideway, the maximum temperature difference is about 2°C, which is reduced about 50% compared without optimization of the guideway. Comparing with Figure 16(a) and Figure 16(b), the temperature field of the guideway with heat transfer system is more uniform than that without optimized.

Figure 16(c) shows the thermal deformation of the guideway before optimized, Δ1 to Δ5 are the thermal deformations measured by eddy current displacement sensors D1 to D5. The maximum thermal deformation along the Y-direction is 14.8 μm which occurred in the middle of the guideway. Except for the thermal deformations of both ends of the guideway, the thermal convex deformation of the guideway is 7.6 μm.

Figure 16(d) shows thermal deformations of the guideway with heat transfer system, the maximum thermal deformation along the Y-direction is 15.8 μm which occurred in the middle of the guideway. Except for the thermal deformations of both ends of the guideway, the thermal convex deformation of the guideway is 3.7 μm, which is reduced about 50% compared without optimization of the guideway. Comparing with Figure 16(c) and Figure 16(d), the thermal equilibrium time is also reduced significantly when the guideway is optimized using the heat transfer system. The experimental results show that the conservation of energy-based thermal optimization method can effectively reduce the thermal convex deformation of the guideway. It is of significance for improving the machining accuracy of machine tool.

5. Conclusions

An optimization method for thermal convex deformation of machine tools' guideway is proposed in this paper. The output and input heat are determined according to the conservation of energy, the structure and contact area of the heat transfer system is designed. Based on the numerical simulation and the experimental results, the following conclusions can be drawn.

(1) A heat transfer system is designed based on the principle of conservation of energy, which can balance the temperature field and reduce the thermal convex deformation of the guideway significantly.

(2) The structure and contact area of the heat transfer system are designed according to the subdivision of output and input heat ratio.

(3) The temperature distribution along the axial direction of the guideway and the linear fitting of the temperature rise is used to determine the output and input heat ratio of the guideway.

(4) A thermal behavior testing platform of guideway is designed which can measure the temperature and thermal deformation of the guideway conveniently.

(5) The experimental results show that the temperature difference and the thermal convex deformation of the guideway is reduced about 50% using the thermal optimization method. It is of significance for improving the machining accuracy of machine tool.

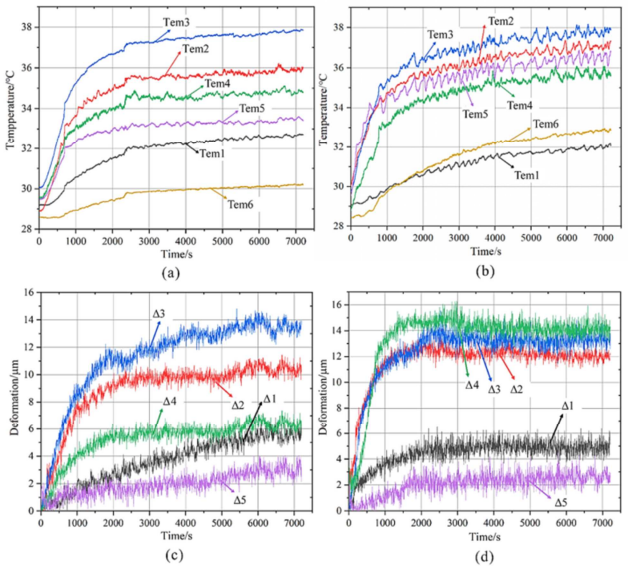

Figure 16. *Experimental results, (a) Temperature rise of guideway before optimized, (b) Temperature rise of guideway with heat transfer system, (c) Thermal deformation along Y-direction before optimized, (d) Thermal deformation along Y-direction with heat transfer system.*

Figure 16. Tem1 to Tem6 are the temperature rises of the guideway, Δ1 to Δ5 are the thermal deformations of the guideway.

6. Recommendations for Future Work

In this study, the temperature field of the guideway is optimized based on the conservation of energy, and a fast heat conduction system is designed to reduce thermal convex deformation. With the development of additive manufacturing technology, the complex structures of the heat transfer system can be machined. Therefore, the proposed method is of great significance to improve the accuracy of machine tools.

Acknowledgements

This paper is sponsored by the "Technology of on-line monitoring system for thermal characteristics of NC machine tools" (No. H2019304021); the "Project funded of Shanghai science committee- Precision technology and its application for five-axis machine tool based on the real-time compensation" (NO. J16022).

References

[1] Bryan J (1990) International status of thermal error research. Annals of the CIRP, 39 (2): 645-656.

[2] Yun W-S, Kim S-K, Cho D-W (1998) Thermal error analysis for a CNC lathe feed drive system. Int J Mach Tools Manuf 39 (1): 1087-1101.

[3] Fan KG, Yang JG, Yang LY (2014) Unified error model based spatial error compensation for four types of CNC machining center: part II-unified model based spatial error compensation. Mech Syst Signal Pr 49: 63-76.

[4] Jiang H, Fan KG, Yang JG (2014) An improved method for thermally induced positioning errors measurement, modeling, and compensation. Int J Adv Manuf Technol 75: 1279-1289.

[5] Feng W, Li Z, Gu Q et al (2015) Thermally induced positioning error modelling and compensation based on thermal characteristic analysis, Int J Mach Tools Manuf 93: 26-36.

[6] Barakat NA, Elbestawi MA, Spence AD (2000) Kinematic and geometric error compensation of a coordinate measuring machine. Int J Mach Tools Manuf 40: 833-850.

[7] Chen L (2009) Kinematics modeling and post-processing method of five-axis CNC machine, 2009 First International Workshop on Education Technology and Computer Science 1: 300-303.

[8] Mori M, Mizuguchi H, Fujishima M et al (2009) Design optimization and development of CNC lathe headstock to minimize thermal deformation. CIRP Ann Manuf Technol 58 (1): 331-334.

[9] Ge Z, Ding X (2018) Design of thermal error control system for high-speed motorized spindle based on thermal contraction of CFRP. Int J Mach Tools Manuf 125 (Supplement C): 99-111.

[10] Fan KG, Gao R, Zhou H et al (2020) An optimization method for thermal behavior of high-speed spindle of gear form grinding machine. Int J Adv Manuf Technol 107: 959-970.

[11] Xia CH, Fu JZ, Lai JT et al (2015) Conjugate heat transfer in fractal tree-like channels network heat sink for highspeed motorized spindle cooling. Appl Therm Eng 90: 1032–1042.

[12] Li F, Gao J, Shi X et al (2017) Investigation on heat transfer performance of loop thermosyphon for inner cooling of motorized spindle. J Xi'an Jiaotong Univ 51 (7): 90–97.

[13] Guo X, Hu Y, Xia J et al (2007) Study on thermal deformation of machine tools' slide guide based on FEA. Modular Machine Tool & Automatic Manufacturing Technique 3 (1): 8-12.

[14] Zeng H, Zhao D, Zeng G et al (2012) Study on thermal deformation of numerical control lathe's slide guide based on Ansys. Machinery Mesign & Manufacture 8: 195-197.

[15] Kang Y, Chang C, Chu M et al (2006) Estimation of thermal deformation in machine tools using the hybrid autoregressive moving-average-neural network model. P I Mech Eng B-J Eng 220 (8): 1317-1323.

[16] Hiroshi T, Yoshiyuki K, Teppei A et al (2007) Approximation of thermal deformation behaviour of a machine tool to improve its process precision. Key Engineering Materials 356 (1): 181-184.

[17] Li H, Ying X (2011) Approximate model method in optimization calculation of thermal error of machine tool guideway. Chinese Journal of Mechanical Engineering (2): 423-427.

[18] Hao Z, Kaiguo F, Rui G (2020) Fast heat conduction-based thermal error control technique for spindle system of machine tools. Int J Adv Manuf Technol 107: 653-666.

[19] Song S, Yovanovich M (1988) Relative contact pressure-Dependence on surface roughness and Vickers microhardness. J Thermophys Heat TR 2 (1): 43-47.